JOURNAL OF CATALYSIS 49, 18–41 (1977)

Interaction of Nitrogen with Iron Surfaces
I. Fe(100) and Fe(111)

F. BOZSO,[1] G. ERTL, M. GRUNZE,[2] AND M. WEISS

Institut für Physikalische Chemie, Universität München, München, Germany

Received December 12, 1976; revised April 18, 1977

The adsorption of N_2 on clean Fe(100) and Fe(111) single-crystal surfaces was studied in the temperature range 140–1000 K by means of Auger electron spectroscopy (AES), low-energy electron diffraction (LEED), ultraviolet photoelectron spectroscopy (UPS), thermal-desorption spectroscopy (TDS) and work-function measurements ($\Delta\phi$). Above room temperature, only dissociative adsorption takes place, leading to increases in work function of 0.33 and 0.25 eV on Fe(100) and (111), respectively, and is mainly identified with UPS by the appearance of a chemisorption level derived from N2p-states at about 5 eV below the Fermi level. At 500 K, the initial rate of adsorption is faster by about a factor of 20 on the (111) plane, the initial sticking coefficient, however, being very small (10^{-7}–10^{-6}) on both surfaces. The initial activation energies for adsorption are about 5 and 0 kcal/mole on Fe(100) and Fe(111), respectively, and increase with coverage in both cases. The mean activation energies for desorption were estimated to be 58(100) and 51 kcal/mole (111), so that nearly equal values for the strength of the M–N bond result. A simple ordered c2 × 2 structure is formed on Fe(100) which is completed at $\theta = 0.5$ and for which a model is proposed wherein the N atoms are located in fourfold sites on the unreconstructed Fe(100) surface, leading to a configuration similar to that in the (002) plane of (fcc) Fe_4N. Several independent observations strongly indicate that the Fe(111) surface reconstructs. A whole series of complex LEED patterns (depending on N bulk and surface concentrations and on the conditions of heat treatment) is formed with this plane which are interpreted in terms of the formation of hexagonal layers of "surface nitrides" which have a thickness of about 2 atomic layers and most probably are related to the (111) plane of Fe_4N. Desorption of N_2 (being found to be a first-order rate process) is regarded as equivalent to the decomposition of the "surface nitrides." The close similarity to the kinetics of decomposition of (bulk) Fe_4N indicates identical mechanisms for both processes. Although the bulk solubility of N is very small under the chosen experimental conditions, this process interferes with the adsorption and desorption measurements and was analyzed in some detail, mainly by $^{14}N/^{15}N$ isotopic exchange. Evidence for the existence of a weakly bound (probably molecular) species was found with Fe(111) only at the lowest temperatures (140 K) and under a steady-state pressure of 4×10^{-4} Torr of N_2. This species causes a decrease in the work function and is rapidly pumped off. Its adsorption energy is estimated to be in the range between 5 and 10 kcal/mole.

1. INTRODUCTION

In spite of numerous investigations during the past decades, the mechanism of ammonia synthesis on iron catalysts is not yet clear (*1*). Although it is well established that nitrogen is present on the catalyst surface under reaction conditions, the nature of interaction of this molecule with Fe surfaces is still a controversial problem. Temkin and Pyzhev (*2*) formulated a rate equation for ammonia synthesis under the

[1] Present address: Gas Kinetics Research Group, Hungarian Academy of Sciences, Szeged, Hungary.

[2] Present address: Freie Universität Berlin, Institut für Physikalische Chemie und Quantenchemie, Berlin, Germany.

ISSN 0021-9517

assumption that dissociative nitrogen adsorption is rate determining, which proved to describe successfully the experimental data. Later studies however led to the conclusion that adsorbed hydrogen is involved in the rate-determining step: Tamaru (*3*) observed that the uptake of nitrogen is accelerated by the presence of adsorbed hydrogen, and Ozaki *et al.* (*4*) reported an H/D isotope effect for the rate of ammonia synthesis. Nevertheless, at present, it is again commonly believed (*1*) that chemisorption of nitrogen is the slowest step in ammonia synthesis. This assumption is supported by the fact that the other compounds involved (H_2, NH_3) are adsorbing and desorbing very fast under reaction conditions.

Conclusions about the chemical nature of the chemisorbed and catalytically active nitrogen species are contradictory in the literature: Kummer and Emmett (*5*) as well as Morikawa and Ozaki (*6*) concluded from their isotopic exchange experiments that, above 350°C, only atomic nitrogen is present on the surface. According to Takezawa and Emmett (*7*), between 130 and 300°C, a considerable amount of nitrogen is held in a molecular from. Evidence for molecularly chemisorbed nitrogen was also found in a series of other investigations (*8–11*) leading Brill (*12*) to the formulation of a rate equation for the kinetics of ammonia synthesis based on the assumption of hydrogenation of molecular nitrogen. [There is also clear evidence for weakly adsorbed molecular nitrogen which desorbs below room temperature and which obviously is not identical with the more tightly bound species involved in the reaction (*13*).] On the other hand, Scholten *et al.* (*14*) concluded that, even at 20°C, atomic nitrogen is the strongly adsorbed species formed by interaction of N_2 with iron.

Another important question concerns the nature of the active surface: Brill *et al.* (*11*) interpreted their results with Fe field-emitter tips in terms of only the (111) plane being able to chemisorb molecular nitrogen and, therefore, being catalytically active. Recently very careful studies, including Mössbauer spectroscopy with small iron particles by Dumesic *et al.* (*15*, *16*), showed that ammonia synthesis is a structure-sensitive reaction, and that nitrogen may induce reconstruction of the iron surface. It was concluded that so-called C_7 sites [as present on the (111) plane] are more active than others. In addition, the possible role of formation of surface nitrides is not yet clear. Although bulk iron nitride is thermodynamically unstable under reaction conditions, the possibility of the existence of surface compounds of this type is discussed several times in the literature (*8*, *17–19*).

So far, only very few experiments were performed with 'clean' surfaces under UHV conditions (*20*), and, to our knowledge, no results of studies on the interaction of N_2 with Fe single-crystal surfaces were published from other laboratories. The aim of the present extended work was an investigation of the chemical, structural, and kinetic features of N_2 interaction with iron single-crystal surfaces of different orientation. The applied techniques included low-energy electron diffraction (LEED), Auger electron spectroscopy (AES), thermal desprption spectroscopy (TDS), ultraviolet photoelectron spectroscopy (UPS), and work-function measurements. Some preliminary results with Fe(100) have already been published (*21*). The present report is concerned with the Fe(100) and Fe(111) surfaces. The results of experiments with (110) and polycrystalline Fe surfaces will be published later, as well as studies on the decomposition of NH_3 and on the interaction with $H_2 + N_2$.

2. EXPERIMENTAL

Most of the experiments were performed within a stainless steel standard UHV sys-

tem (base pressure $<10^{-10}$ Torr) which was equipped with a four-grid LEED optics, an additional glancing-angle electron gun for AES, and facilities for measuring changes of the work function by means of the vibrating-condensor technique. A quadrupole mass spectrometer served for monitoring the composition of the gas atmosphere and for recording thermal desorption spectra. Photoemission spectra were taken within a separate combined UPS–LEED system which is described elsewhere (*22*). All reported spectra were excited by He II-resonance radiation ($h\nu$ = 40.8 eV).

The samples consisted of cylindrical disks (8 mm in diameter, 1 mm thick) which, after proper crystallographic orientation to within 1°, were cut from a single-crystal rod (purity 99.99%) by means of spark erosion and carefully mechanically polished. They were then spot-welded between two parallel thin tungsten wires which were themselves fixed to Mo rods mounted on the axis of a manipulator. A chromel–alumel thermocouple spot-welded on the rear of the sample served for measuring the temperature which could be varied between 135 and 1000 K. Cooling the sample below room temperature was performed by a cold finger filled with liquid nitrogen.

Cleaning the surfaces was found to be a very difficult and tedious task which is described in some detail in Ref. (*21*). In the presence of larger amounts of impurities such as O and C, the (111) surface showed a strong tendency for thermal facetting. (In fact, one of the samples was destroyed in this way.) High-temperature argon ion bombardment over long periods of time, therefore, had to be performed rather carefully in order to remove all the impurities segregating from the bulk to the surface. The Auger spectra of the "clean" surfaces exhibited no contaminants except for less than a few percent of a monolayer of carbon. There was no indication that such small amounts of impurities influenced the results. Considerable care also had to be taken with respect to impurities in the residual gas atmosphere during the large N_2 exposures necessary for the adsorption experiments: CO was observed to adsorb very rapidly and to dissociate easily on the surface. This problem could not be completely eliminated with the UPS apparatus; therefore, smaller N_2 exposures were applied in order to minimize this disturbing effect. The standard UHV system was pumping large amounts of N_2, H_2, and NH_3 over a period of more than a year and, thereby, produced a vacuum in which the CO concentration was completely negligible.

3. RESULTS

3.1 Auger Electron Spectroscopy

The kinetics of nitrogen adsorption was followed primarily by means of AES. The ratio y of the Auger peak for N at 380 eV to that of Fe at 650 eV was used as a measure of the relative surface concentration of nitrogen. As will become evident from other measurements, this assumption is questionable in the case of Fe(111), where reconstruction of the surface region takes place and the term "surface concentration" becomes somewhat ambiguous. No such complication was observed with Fe(100).

The experiments were performed by exposing the samples at fixed temperatures to varying amounts of N_2. Since the sticking coefficient is very low, an N_2 pressure of 4×10^{-4} Torr was usually applied. After exposure, the vacuum system was evacuated into the low 10^{-9}-Torr pressure region prior to switching on the primary electron beam for Auger spectroscopy. Interaction of the electron beam with gaseous N_2 was observed to cause further variations of the surfaces (presumably due to the uptake of atomic nitrogen) which was thus eliminated. On the other hand, there was no indication for noticeable electron beam effects on a chemisorbed nitrogen layer. A

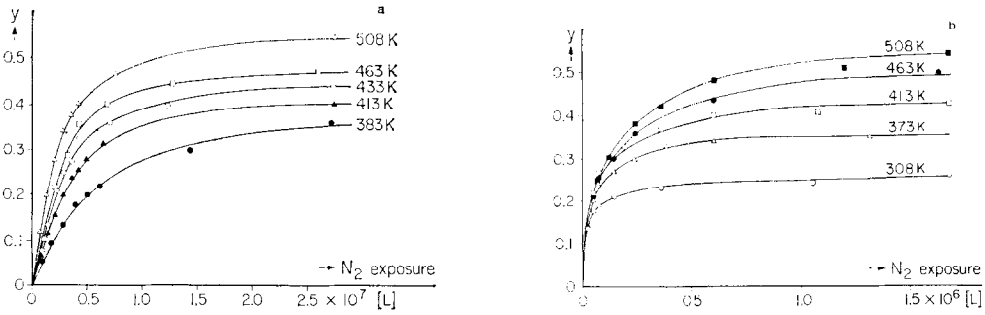

FIG. 1. Rate of nitrogen chemisorption at different temperatures as followed by recording the N:Fe Auger peak-height ratio y as a function of N_2 exposure (1 L = 10^{-6} Torr × sec). (a) Fe(100); (b) Fe(111).

further complication arises from the solubility of nitrogen in the bulk. The equilibrium bulk concentration n_b (in weight percent) at 1 atm of N_2 is given by (*23*)

$$n_b = 0.098 \exp(-\Delta H_s/RT),$$

where ΔH_s (= +7.2 kcal/mole) is the enthalpy for the reaction

$$\tfrac{1}{2}N_{2,gas} \rightleftharpoons N_b.$$

Even though n_b is rather small (6×10^{-6}% at 100°C, 2.4×10^{-3}% at 700°C) it cannot be assumed that the segregation equilibrium

$$N_{surf.} \rightleftharpoons N_{bulk}$$

will always be automatically established. Unfortunately, the available experimental techniques did not allow the determination of the concentration profile of bulk nitrogen. [The segregation equilibrium, starting from known bulk concentrations, is presently being studied by Grabke (*24*).] The influence of N_2 pretreatment of the Fe(100) sample on the adsorption kinetics was described in some detail in Ref. (*21*). In order to obtain reproducible and comparable conditions, both samples were always pretreated in the same manner: After prolonged interaction with 4×10^{-4} Torr of N_2 at 600 K (which caused nitrogen saturation, at least of the regions near the surface), the surfaces were cleaned by a short argon ion bombardment and subsequently annealed at 600 K for 1 hr.

The formation of tightly bound adsorbed nitrogen layers was observed to occur with Fe(100) above room temperature and with Fe(111) even at 140 K. The variation of the N/Fe Auger signal ratio y, as a function of N_2 exposure at different temperatures, is reproduced in Fig. 1a for Fe(100) and in Fig. 1b for Fe(111). (Note the different scales for the abscissa!) Evidently, the uptake of nitrogen proceeds much faster with the Fe(111) surface. At 508 K, the initial rates of adsorption differ by about a factor of 20 between both planes. Data for Fe(100) between 533 and 783 K are reproduced in Fig. 2: Above 670 K, the bulk diffusion processes and the onset of desorption become important and cause a decrease in the final surface concentration.

Derivation of the activation energy for adsorption E^*_{ad} is only meaningful up to temperatures of about 470 K, where bulk

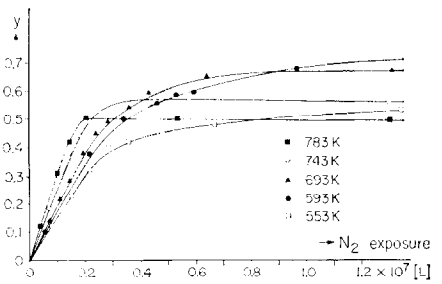

FIG. 2. Rate of nitrogen adsorption (y vs exposure) on Fe(100) at higher temperatures.

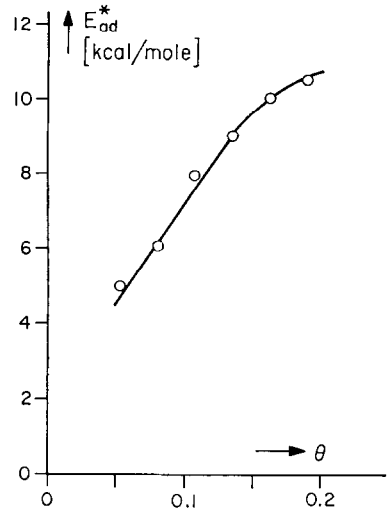

FIG. 3. Variation of the activation energy for N_2 adsorption, E^*_{ad}, on Fe(100) with coverage θ. θ is defined as the ratio of numbers of atoms of N:Fe in the surface layer. Calibration was achieved from $\theta_{max} = 0.5$ as derived from the LEED data.

diffusion may be neglected. The resulting values for E^*_{ad} on Fe(100) are drawn in Fig. 3 as a function of the surface concentration. As will be outlined later, $y = 0.9$ corresponds to $\theta = 0.5$ (as derived from LEED) data, so that a calibration of the relative surface concentration in terms of coverage becomes possible. As can be seen from Fig. 3, E^*_{ad} rises continuously from a value of about 5 kcal/mole to about 10 kcal/mole at $\theta = 0.2$. This result compares well with the findings of Scholten *et al.* (*14*) who derived a similar increase of the activation energy of nitrogen adsorption on Fe catalysts between 20 and 260°C and 7 and 110 Torr of N_2. Since the activation energy increases, the rate of adsorption becomes continuously slower with increasing coverage. This is believed to be the reason why the curves at different temperatures in Fig. 1 apparently do not reach the same saturation coverages. (As outlined before, above 670 K, the equilibrium surface concentration will again be lowered due to the onset of desorption.) The variation of the sticking coefficient with coverage for N_2 adsorption on Fe(100) at different temperatures, as derived from the Auger data, is reproduced in Fig. 4.

The initial activation energy on Fe(111) is apparently vanishingly small. A detailed analysis of the work-function data to be described below indicates that, in this case, E_{ad} varies only between 0.1 and 1 kcal/mole with increasing coverage.

3.2. Thermal Desorption

Because of the phase transition between bcc α-Fe and fcc γ-Fe at 1179 K, thermal desorption experiments were restricted to temperatures below about 1050 K. [The transition temperature may become considerably lower in the presence of dissolved nitrogen (*25*).] Spectra were recorded for Fe(111) with a constant heating rate of 10 K/sec, whereas, with the Fe(100) sample, this parameter varied between 6 and 10 K/sec, depending on temperature. As expected, severe complications arose in the proper analysis of the spectra due to interference with bulk diffusion as well as desorption of the nitrogen initially dissolved in the bulk. As a consequence, normal desorption spectra exhibited no distinct maximum but only a continuous increase in N_2 desorption above ca. 750 K, due to superposition of surface and bulk effects. In order to discriminate between

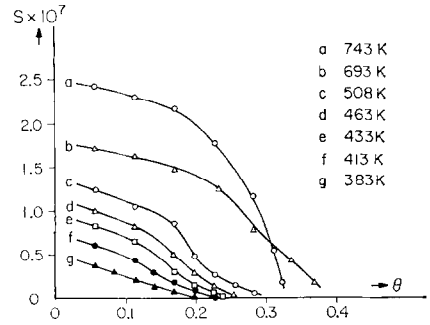

FIG. 4. Variation of the sticking coefficients for N_2 adsorption on Fe(100) with coverage at different temperatures.

these effects, the following procedure was applied.

The sample was exposed to 4×10^{-4} Torr of $^{28}N_2$ at 700 K for 12 hr. As a result, the subsurface layer was saturated with dissolved ^{14}N. Subsequently, the surface was Ar^+ ion bombarded at 320 K until no nitrogen could be detected on the surface by means of AES. (Since the equilibrium bulk concentrations are far below 1%, AES is not able to detect such small quantities of N present in the subsurface region.) After briefly annealing, the surface was exposed to 4×10^{-4} Torr of $^{30}N_2$ until the desired surface concentration (as monitored by AES) was reached. Subsequent thermal desorption spectra were recorded with respect to $^{30}N_2$. As can be seen from Fig. 5, pronounced maxima now result, and these are ascribed to N_2 desorbing from the surface layer. But, even under these conditions, a small amount of ^{15}N diffused into the bulk and reappeared in the desorption spectrum as a small shoulder on the high-temperature side of the main peak. The effects of nitrogen exchange between surface and bulk will be discussed in some more detail with the results for Fe(111).

Figure 5 represents a series of $^{30}N_2$ desorption traces from Fe(100) with varying surface concentrations. As can be seen, the maximum temperature is shifted by about 50 K toward lower temperatures with increasing coverage. This effect is much too small to account for second-order desorption kinetics from an energetically uniform adsorbate layer. Instead, it is believed that desorption essentially follows first-order kinetics, and that the temperature shift is due to a slightly decreasing heat of adsorption with increasing coverage. Assuming a normal frequency factor of 10^{13} sec^{-1}, the activation energy for N_2 desorption from Fe(100) is estimated to be about 58 kcal/mole. In spite of the apparent first-order desorption kinetics, nitrogen is certainly not molecularly chemisorbed but is present on the surface in atomic form, as is evident from various other observations. It was recently observed also with other systems (*26*, *27*) that N_2 desorption from a dissociatively adsorbed layer obeys first-order kinetics which, therefore, seems to be a general feature and will be discussed later.

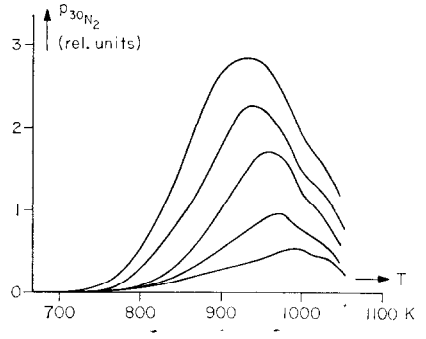

FIG. 5. Thermal desorption spectra for $^{30}N_2$ desorbing from Fe(100) at various initial coverages. The subsurface region was saturated with ^{14}N (see text).

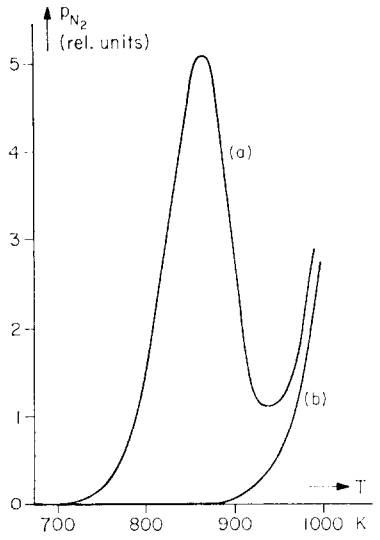

FIG. 6. Thermal desorption spectra from Fe(111). (a) First Run; (b) second run.

From a Fe(111) surface, chemisorbed nitrogen desorbs with a maximum rate at a temperature roughly about 100°C lower than that from Fe(100). The activation energy for desorption is estimated to be about 51 kcal/mole. As becomes evident from Fig. 6, desorptions from surface and

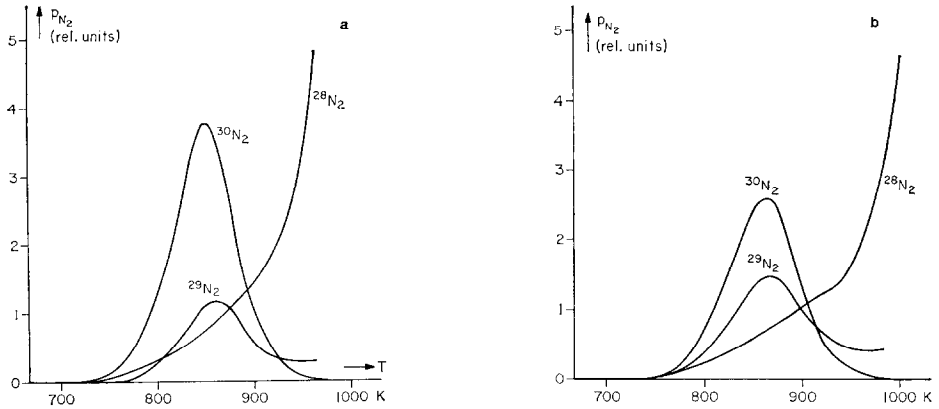

FIG. 7. Thermal desorption spectra for $^{28}N_2$, $^{29}N_2$, and $^{30}N_2$ desorbing from Fe(111) (pretreatment, see text). Five (a) and sixty (b) minutes of annealing at 640 K prior to desorption.

bulk states may now clearly be distinguished from each other. In this experiment, the sample was exposed only to $^{28}N_2$, and the desorbing nitrogen was monitored mass spectrometrically at $m/e = 14$. Curve a was taken from a surface with a certain nitrogen coverage. Following heating to 1000 K, the sample was cooled, and, subsequently spectrum b was recorded. Prior to this second run, AES revealed that the surface concentration of nitrogen was negligible. This result indicates that the pressure burst above 900 K arises from nitrogen segregating during the temperature rise from the bulk to the surface and subsequently desorbing, whereas the peak in curve a arises from a species already present on the surface at the beginning of the experiment.

The following measurements were performed by applying the same $^{28}N_2$–$^{30}N_2$ pretreatment as described above for Fe(100). Figure 7a represents thermal desorption spectra for masses 28, 29, and 30 taken in three separate runs with identical pretreatments. Since prior to adsorption of $^{30}N_2$ AES revealed no presence of nitrogen on the surface (which could have segregated from ^{14}N dissolved in the bulk), the subsequent observation of desorption of $^{28}N_2$ and $^{29}N_2$ in the temperature range of "surface" nitrogen must be ascribed to an isotopic exchange process between bulk and surface after formation of the adsorbed layer. As a consequence, the ratio of amounts of desorbing molecules with different isotope compositions should be dependent on the annealing time. Whereas with Fig. 7a the sample was annealed for 5 min at 640 K prior to desorption, in Fig. 7b, the results are reproduced for a 60-min annealing at the same temperature: The amount of desorbing $^{30}N_2$ decreased, whereas $^{29}N_2$ increased. The amount of $^{28}N_2$ desorbing from the surface in this case is even slightly smaller than that shown in Fig. 7a. This is ascribed to the fact that, during the longer annealing period, some nitrogen from the subsurface region was diffusing still further into the bulk. The total amount of N_2 desorbing in the surface-nitrogen temperature region was also smaller in the second case, although AES indicated identical concentrations.

This apparent disagreement between surface concentrations determined by AES and by thermal desorption spectroscopy became even more evident in the following sets of experiments (Fig. 8): Spectra a–d were recorded after adsorbing N_2 at Fe(111) at 313 K. The Auger y values ranged between 0.11 and 0.27, as indicated. Curves e–g were recorded after adsorption at 640 K, the y values again being in the

same range. If, for example, curves a and e or c and f are compared with each other, it becomes evident that the higher adsorption temperature leads (at identical Auger peak height ratios) to a release of a considerably higher amount of N_2 in the temperature range of surface nitrogen. The conclusion is that AES probes (with constant sensitivity) a smaller sample depth than TDS. As will become evident from the LEED observations, high-temperature treatment of Fe(111) with N_2 causes the surface to reconstruct, and, therefore, the corresponding thermal desorption spectra, e–g, are described in terms of decomposition of a "surface nitride" (exhibiting a thickness of a few atomic layers), rather than by desorption from the top of an unreconstructed surface.

This effect was studied more quantitatively in a separate set of thermal desorption experiments. In this case, exposure only to $^{28}N_2$ (7×10^5 L at varying temperatures) was performed in order to avoid complications from isotopic exchange reactions. The relative desorbing amounts (within the temperature range of the "surface" maximum) m were determined from the areas below the desorption traces, $m = \int p dt$. The resulting data are reproduced in Table 1 together with the corresponding y values from AES and the work-function changes $\Delta\phi$ (as described in the next section). This table also contains the relative ratios y/m and $\Delta\phi/m$, referred to 318 K $\triangleq$ 100%. If adsorption and desorption were confined to identical sites on the surface irrespective of the temperature of exposure, both ratios should remain constant which obviously is not the case. Instead, y/m decreases continuously with increasing adsorption temperature. This effect is even more pronounced with the ratio $\Delta\phi/m$. These results show that, with Fe(111), the determination of the "surface" concentration of nitrogen is somewhat ambiguous and depends on the applied technique: Obviously, TDS probes all N_2 molecules desorbing in the considered temperature range; the sensitivity of AES is largest for the topmost atomic layer and decreases rapidly with the depth of penetration of the nitrogen atoms in the solid; $\Delta\phi$ reflects the dipole moment at the surface and, consequently, is the most surface-sensitive method. The conclusion is that, with

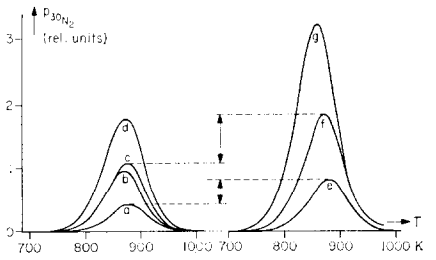

FIG. 8. Thermal desorption spectra from Fe(111). Spectra a–d: adsorption at 313 K; spectra e–g: adsorption at 640 K.

	y Values from AES						
	a	b	c	d	e	f	g
y	0.11	0.16	0.20	0.27	0.11	0.21	0.34

TABLE 1

Exposures of Fe(111) to 7×10^5 L of N_2 at Varying Temperatures

	Adsorption temperature (K)						
	318	373	413	463	593	643	688
y from AES	0.28	0.36	0.43	0.45	0.48	0.49	0.50
m from TDS (relative units)	58	82	93	106	118	124	140
$\Delta\phi$ [mV]	165	208	257	245	240	232	235
y/m (%) (318 K $\triangleq$100%)	100	92	96	88	85	83	80
$\Delta\phi/m$ (%) (318 K $\triangleq$100%)	100	89	97	87	71	66	59

increasing temperature of exposure, continuously increasing amounts of nitrogen are "buried" below the topmost atomic layer. This agrees well with the conclusions from the LEED experiments which indicate continuous structural transformations involving reconstruction of the Fe(111) surface with increasing temperature and nitrogen concentration.

With both single-crystal planes no indication of the existence of a less tightly bound molecular nitrogen species was found. Even after exposure at 140 K and subsequent evacuation, no additional state was detected in the thermal desorption spectra. As becomes evident from the just described results with Fe(111), isotopic mixing of ^{14}N and ^{15}N and the desorption of $^{29}N_2$ can be reconciled only with the existence of atomic nitrogen. In order to confirm this conclusion also for Fe(100), this surface was exposed to a 1:1 mixture of $^{28}N_2$ and $^{30}N_2$ at 373 and 700 K. In both cases, desorption of $^{29}N_2$ with the same maximum temperatures as for $^{28}N_2$ or $^{30}N_2$ was observed, again indicating dissociative adsorption.

Since with Fe(111) the "surface" and bulk desorption maxima are well separated on the temperature scale, in this case the isotope exchange on the surface could be completely separated from that in the bulk: Fe(111) was exposed at 140 K to a 1:1 mixture of $^{30}N_2$ and $^{28}N_2$. The amounts of $^{30}N_2$ and $^{29}N_2$ desorbing with a peak maximum at 900 K exhibited a ratio of 2:1, as is expected for the case of complete isotopic equilibration.

3.3 Variation of the Work Function

Adsorption of N_2 on Fe(100) above room temperature was observed to cause a continuous increase in the work function until a saturation value $\Delta\phi_{sat} = 0.33 \pm 0.02$ eV was reached. $\Delta\phi$ was found to be proportional to the corresponding y value from AES, irrespective of adsorption temperature or coverage. This result indicates that, with this plane, both techniques directly yield the relative surface concentration. The constancy of the adsorbate dipole moment supports the conclusion that, with this surface, no reconstruction, but only formation of a regular overlayer takes place.

With Fe(111), structural transformations of the surface region are again reflected in the more complicated behavior of the $\Delta\phi$ data: As already outlined in Section 3.2, the ratios $\Delta\phi/m$ or $\Delta\phi/y$ are no longer constant, but depend on the heat treatment of the sample. $\Delta\phi$ attains a maximum value of about 0.25 eV. The variation in $\Delta\phi$ with exposure at different temperatures is shown in Fig. 9. (Note that the exposure scale is considerably enlarged with respect to Fig. 1b.) For the sake of clarity, data from low- and high-temperature ranges are displayed separately. Up to about 500 K, the initial slope $d\Delta\phi/dt$ increases with temperature, from which a very small initial activation energy for adsorption $E^*_{ad} \approx 0.1$ kcal/mole is derived. With increasing coverage, this quantity increases, as already indicated by the AES data of Fig. 1b, but no quantitative evaluation was made. The initial rate of $\Delta\phi$ increase passes through a maximum at around 550 K and decreases with further increasing temperature as can be seen from Fig. 9b. Above ca. 410 K, $\Delta\phi$ passes with increasing exposure through a flat maximum, which shifts toward smaller exposures with increasing temperature. Above about 550 K, the saturation value of $\Delta\phi$ decreases slightly. All these data suggest that adsorption is superimposed by another process which is associated with a slight decrease in the work function and the rate of which increases with temperature. Obviously, this effect is again correlated with reconstruction of the surface region.

Some experiments were performed at the lowest attainable temperatures (140 K) in order to discover eventually a weakly bound molecular species. With Fe(100), even under a steady-state pressure of 10^{-4} Torr

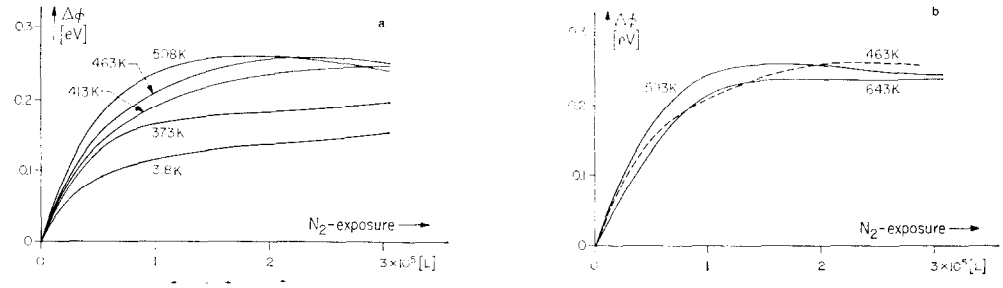

FIG. 9. Variation of the work function $\Delta\phi$ of Fe(111) with N_2 exposure at different temperatures. (a) 318–508 K; (b) 463–643 K.

of N_2, there was no evidence for such a species. If present at all, its equilibrium concentration under these conditions would be too small to cause a noticeable variation in the work function. A different effect was observed with the (111) plane (Fig. 10): Exposure to 4×10^{-4} Torr of N_2 at 140 K causes the work function to increase continuously. Surprisingly, evacuation of the vacuum chamber caused a further $\Delta\phi$ rise by about 40 mV. Readmission of N_2 now leads to a decrease in the work function; the $\Delta\phi$ changes due to gas exposure and evacuation occur fairly rapidly and are completely reversible. The electropositive species which is pumped off is believed to be weakly adsorbed molecular nitrogen. After final evacuation, a relative surface concentration $y = 0.12$ of strongly bound nitrogen was detected by AES, which means that dissociative adsorption also takes place at this low temperature, giving rise to the net $\Delta\phi$ increase. From the fact that the weakly bound molecular species is readily pumped off at 140 K, but on the other hand is present in a measurable equilibrium concentration under an N_2 pressure of 4×10^{-4} Torr, it is roughly estimated that its adsorption energy is between 5 and 10 kcal/mole.

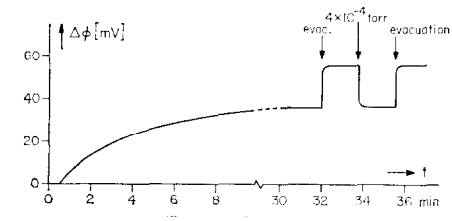

FIG. 10. Variation of the work function $\Delta\phi$ of Fe(111) at 140 K with time after introduction or evacuation of 4×10^{-4} Torr of N_2.

3.4. *Low-Energy Electron Diffraction*

As already outlined in Ref. (*21*), N_2 chemisorption on Fe(100) causes only the formation of a c2 × 2 structure, whereby the LEED pattern exhibits rather sharp "extra" spots already at relatively low coverages, provided that the temperature is high enough to provide the necessary surface mobility of the adsorbed particles (Fig. 11). This observation suggests the formation of

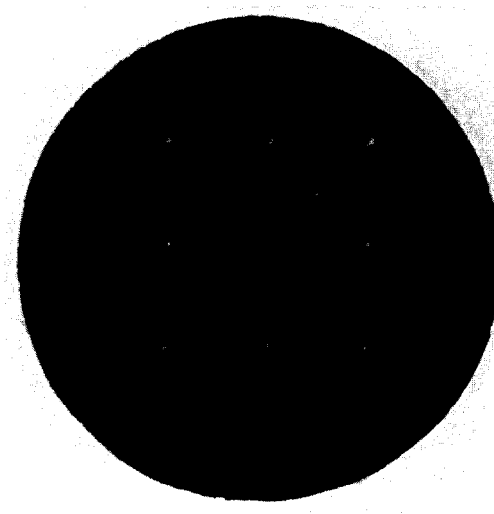

FIG. 11. c2 × 2 LEED pattern on Fe(100) formed after N_2 adsorption (U = 156 V).

islands (initially separated from each other by bare parts of the surface) due to the attractive interactions between next-nearest neighbors. Intensity measurements of the half-order spots at fixed electron energy as a function of temperature indicated an order–disorder transition at about 720 K, i.e., about 50 K below the onset of desorption. Disorder could also be achieved by partial desorption and subsequent quenching: A completely covered surface ($y = 0.9$) was briefly heated to 870 K so that the relative surface concentration dropped to $y = 0.6$, and, subsequently, the sample was cooled to room temperature. The c2 × 2 LEED pattern had completely disappeared but could be restored by annealing the sample at 620 K. Obviously, a temperature in this range is necessary to overcome the activation barrier for surface diffusion. Measurements of the I/V curves of the specular LEED beam for the clean and nitrogen-covered Fe(100) surfaces revealed no shifts in the energies of the primary Bragg maxima, which is probably a hint that no expansion or reconstruction of the topmost atomic layers is caused by nitrogen adsorption. Of course a definite answer to this question may only be obtained by a dynamic intensity analysis, but all other measurements also indicate that no reconstruction occurs with this plane.

It must be mentioned that interaction of N_2 with Fe(100) under the influence of the electron beam causes a splitting of the spots from the c2 × 2 structure. It is assumed that this effect is caused by gaseous N atoms which are formed by electron impact and may cause a structural transformation of the adsorbate layer. In order to avoid this artefact, all LEED and AES observations were made only after evacuating the vacuum system.

The behavior of the Fe(111) surface was much more complex and revealed the formation of a whole series of ordered structures. The LEED pattern from the clean surface exhibits the normal diffraction spots from a (111) plane. Nitrogen adsorption below 410 K caused the intensity of these spots to gradually decrease, whereas the brightness of the background increased. This result indicates the formation of a disordered adsorbate layer.

At sample temperatures between 410 and 470 K, formation of a 3 × 3 structure (LEED pattern of Fig. 12a) was observed to appear at relatively low surface concentrations ($y = 0.1$–0.15) and to disappear with increasing coverage. The full sequence of ordered structures, 3 × 3 (Fig. 12a), $19^{\frac{1}{2}} \times 19^{\frac{1}{2}}$ R 23.4° (Fig. 12b), $21^{\frac{1}{2}} \times 21^{\frac{1}{2}}$ R 10.9° (Fig. 12c), $3(3)^{\frac{1}{2}} \times 3(3)^{\frac{1}{2}}$ R 30° (Fig. 12d), and 2 × 2 (Fig. 12e), was observed upon N_2 adsorption or annealing above 510 K. The formation of these structures could not be unequivocally correlated with distinct ranges of surface concentrations, but was observed to be strongly governed by kinetic (i.e., nucleation) phenomena as well as by bulk nitrogen concentration and type of heat treatment. Very often the LEED pattern was observed to consist of a superposition of diffraction spots from several of these patterns, indicating the formation on the surface of patches with different structures, the average size of which exceeded the coherence width of the LEED electron beam (~100 Å). The $3(3)^{\frac{1}{2}} \times 3(3)^{\frac{1}{2}}$ R 30° structure was always observed to dominate at higher nitrogen concentrations ($y > 0.4$). The $19^{\frac{1}{2}} \times 19^{\frac{1}{2}}$ R 23.4° structure was typically present at $y = 0.35$, but could be transformed into the $21^{\frac{1}{2}} \times 21^{\frac{1}{2}}$ R 10.9° pattern by annealing at 600 K. The 3 × 3 pattern always appeared first and obviously corresponds to the lowest nitrogen concentration. The 2 × 2 LEED pattern was of rather peculiar origin. It appeared if a sample saturated with nitrogen in the bulk, but without any detectable amount of adsorbate on the surface (i.e., no Auger signal from nitrogen), was annealed at 610 K *in vacuo* for about 30 min. Ob-

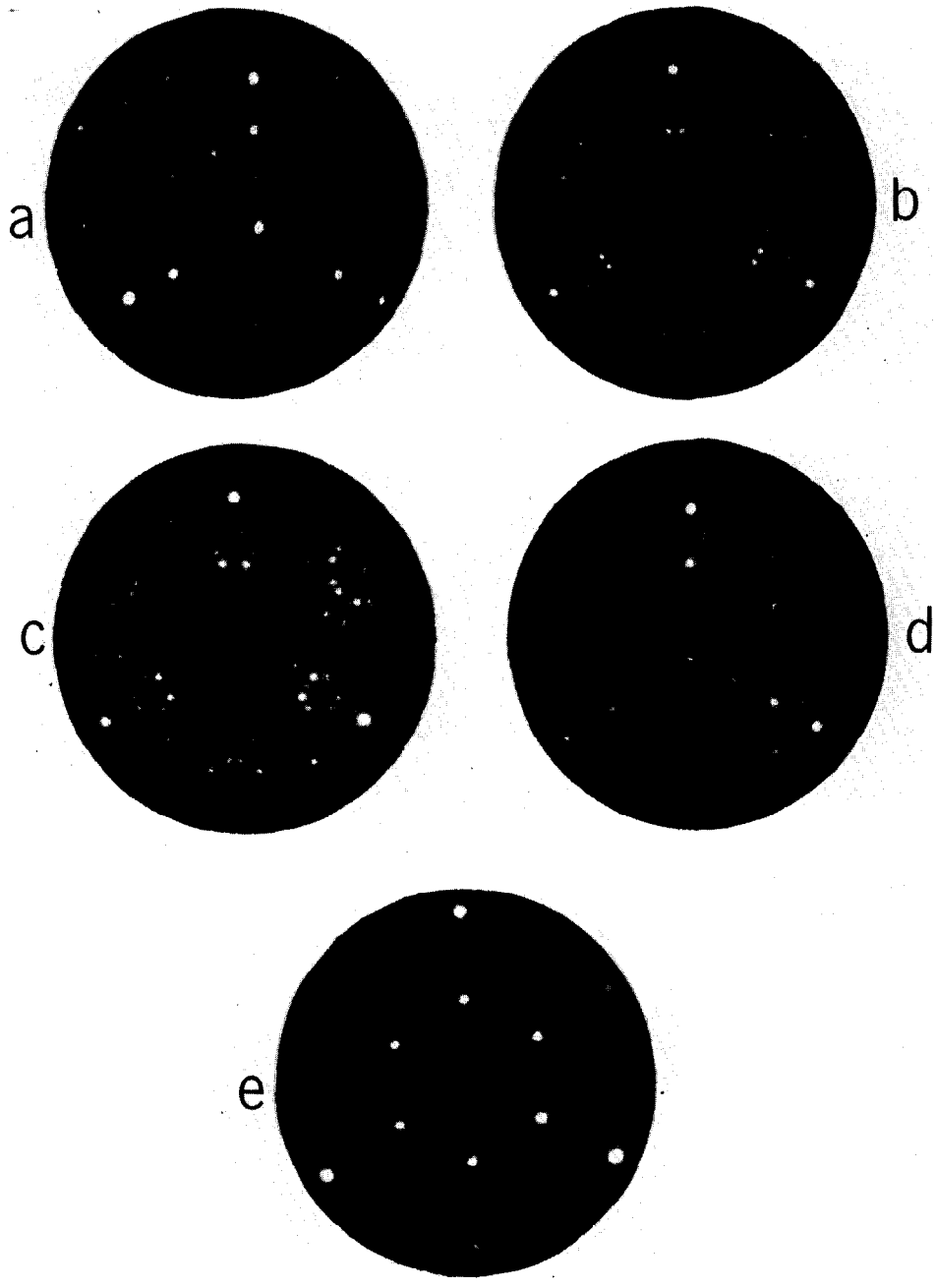

FIG. 12. LEED patterns formed by nitrogen adsorption on Fe(111) (U = 31 V). (a) 3×3 structure; (b) $19^{\frac{1}{2}} \times 19^{\frac{1}{2}}$ R 23.4° structure; (c) $21^{\frac{1}{2}} \times 21^{\frac{1}{2}}$ R 10.9° structure; (d) $3(3)^{\frac{1}{2}} \times 3(3)^{\frac{1}{2}}$ R 30° structure; (e) 2×2 structure.

viously, the clean surface reconstructs into this periodicity under the influence of dissolved nitrogen atoms.

Superpositions from different structures and (in some cases) the occurrence of two domain orientations caused the LEED patterns to appear rather complicated, but a straightforward identification of the struc-

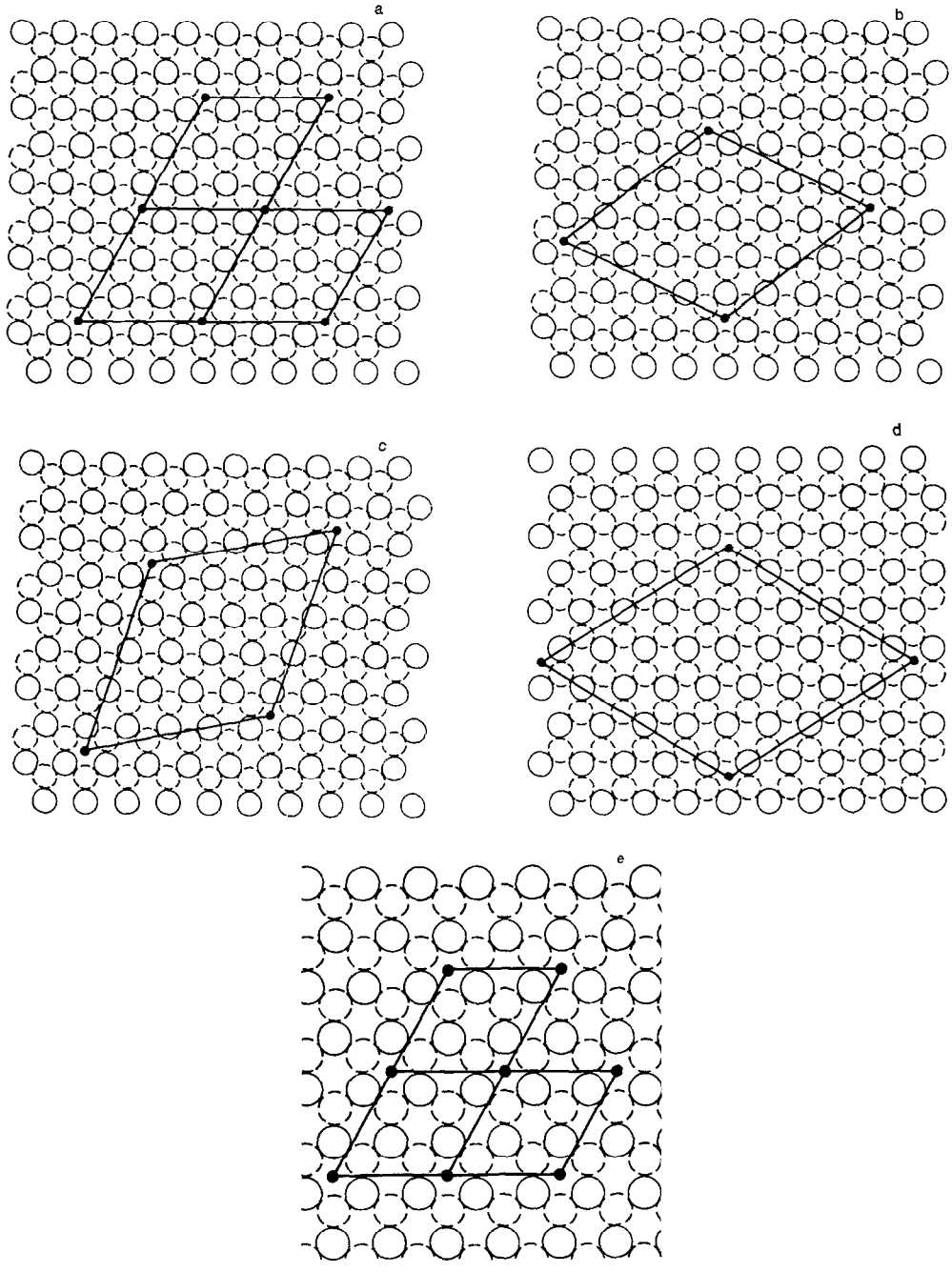

FIG. 13. Unit cells for the nitrogen-induced surface structures as derived from the LEED patterns of Fig. 12 (always only *one* domain orientation). (a) 3×3; (b) $19^{\frac{1}{2}} \times 19^{\frac{1}{2}}$ R 23.4°; (c) $21^{\frac{1}{2}} \times 21^{\frac{1}{2}}$ R 10.9°; (d) $3(3)^{\frac{1}{2}} \times 3(3)^{\frac{1}{2}}$; R 30°; (e) 2×2.

tures and a derivation of their unit cells were possible. These unit cells are reproduced in Fig. 13a–e. Their large size excludes any explanation in terms of simple "in-registry" overlayer structures, but, rather, points toward the formation of co-

incidence lattices connected with a reconstruction of the topmost atomic Fe layers.

3.5. Ultraviolet Photoelectron Spectroscopy (UPS)

UPS was applied mainly as a "fingerprint" technique in order to decide whether the strongly adsorbed species, as studied by the other techniques, is indeed atomic nitrogen instead of molecularly adsorbed N_2. To our knowledge, no photoelectron spectra from adsorbed N_2 are reported so far in the literature. The spectrum from gaseous N_2 exhibits three bands with ionization potentials (I.P.) around 15.5, 17.0, and 18.8 eV with respect to the vacuum level (*28*). Thus, the situation is similar to that for the isoelectronic compound CO (I.P. $=14.0$, 16.9, and 19.7 eV) which, in the chemisorbed state, gives rise to two maxima at about 8 and 11 eV below the Fermi level E_F, which are associated with chemisorption levels derived from the CO $5\sigma + 1\pi$ and 4σ states, respectively (*29*). In the case of molecularly adsorbed nitrogen, analogously, again, two maxima roughly at about 8 and 10 eV below E_F would be expected, taking into account the work function and reasonable estimates for level shifts due to coupling and relaxation effects.

On the other hand, atomic nitrogen was found with Ni (*27*) and Cu (*30*) to produce essentially a single level (besides variations of the emission from the d band) at about 5–6 eV below E_F. Certainly, the situation is not completely different with Fe, so that a clear distinction should be possible.

As already mentioned, the UPS apparatus was observed to have some problems with regard to O_2 and CO partial pressures at high N_2 exposures. Therefore, the experiments were performed with N_2 pressures $<10^{-5}$ Torr and only up to an exposure at which contamination of the surfaces could be neglected. In addition, the spectra after N_2 adsorption were found to be identical to those obtained after

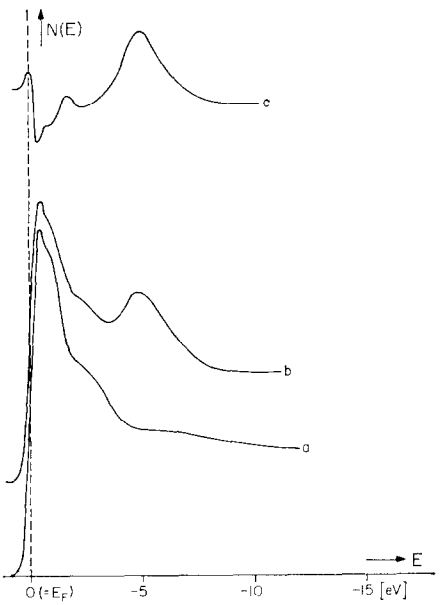

FIG. 14. Ultraviolet photoelectron spectra ($h\nu = 40.8$ eV) from Fe(100). (a) Clean surface; (b) after nitrogen adsorption; (c) difference spectrum (b − a).

decomposition of NH_3 (after removal of H_2, but prior to desorption of N_2). In the latter case, only relatively small exposures were necessary, and the danger of surface contamination was minimized.

With both samples, exposure to N_2 above room temperature caused essentially the appearance of an additional emission maximum around 5 eV below E_F, indicating the atomic nature of the adsorbate. Figure 14 shows spectra ($h\nu = 40.8$ eV) from a clean Fe(100) surface (a) as well as after nitrogen adsorption (b). Curve c represents the difference (b − a), i.e., the variation of emission intensity caused by adsorption. Besides a pronounced peak centered at −5.0 eV, emission from the d band is suppressed, but probably exhibits a second maximum at −1.8 eV.

Similar data for Fe(111) are reproduced in Fig. 15, indicating the appearance of maxima at −1.8 and −5.4 eV. The peak at −5.4 eV was observed to increase continuously with increasing nitrogen concen-

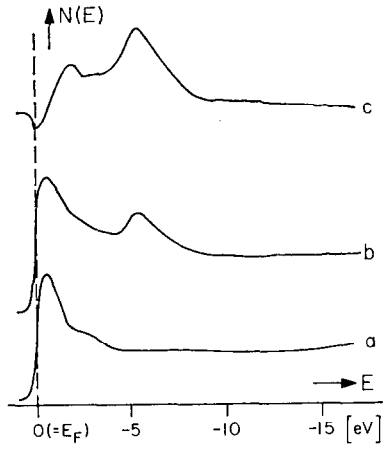

FIG. 15. Ultraviolet photoelectron spectra ($h\nu$ = 40.8 eV) from Fe(111). (a) Clean surface; (b) after nitrogen adsorption; (c) difference spectrum (b − a).

tration, but without any noticeable shift. This indicates that the nitrogen atoms are in essentially identical valence states throughout the various structural transformations occurring at this surface.

Even at the lowest temperature of 140 K and with N_2 pressures $\leq 10^{-5}$ Torr, there was no indication of the appearance of a second type of (molecularly adsorbed) nitrogen. This agrees with the results of the $\Delta\phi$ measurements, whereafter, at this temperature, an electropositive species (presumably $N_{2,ad}$) could be detected only on Fe(111) with N_2 pressures above 10^{-4} Torr. This species is obviously so weakly held that its equilibrium surface concentration at 10^{-5} Torr of N_2 and 140 K is below the detection limits of UPS.

4. DISCUSSION

4.1 Atomic or Molecular Surface Species?

As already briefly mentioned in the Introduction, the chemical nature of nitrogen bound to iron surfaces is a subject of strong discussion in the literature. This question also was not uniquely solved with the few studies so far performed under ultrahigh vacuum conditions: Ponec and Knor (*31*) performed measurements on the change of the electric resistivity and work function of thin evaporated Fe films. At 288 K they observed that $\Delta\phi$ increased by 0.4 eV, whereas it decreased by 0.1 eV upon steady-state exposure to N_2 at 77 K. Qualitatively, these results agree well with the present findings, although (presumably due to the higher low-temperature limit) the electropositive species could only be detected with the Fe(111) face. The authors concluded that, at 77 K, a weakly held (molecular) species predominates, whereas, at room temperature, a tightly bound species exists, presumably in atomic form. Similar results were obtained by Gundry *et al.* (*32*), namely, a $\Delta\phi$ decrease of 0.28 eV at 90 K and an increase of 0.4 eV at 293 K, and again the interpretation was analogous. On the other hand, Wedler *et al.* (*20*) concluded from their thermal desorption and isotope exchange experiments with Fe films that no dissociation occurs at temperatures below 400 K. They observed mainly the desorption of a so-called γ state with a TDS peak temperature at 100 K. Very small amounts of nitrogen (less than a few percent of a monolayer) were also observed to desorb between 200 and 350 K, but these states cannot be associated with the present results with (100) and (111) single-crystal planes. Wedler *et al.* (*20*) determined for their γ state the heat of adsorption calorimetrically to about 5 kcal/mole, which agrees with the lower limit estimated for the adsorption energy of the weakly bound species on Fe(111) in our work. We believe that Wedler *et al.* (*20*) were unable to detect the more tightly bound species by means of calorimetry due to its extremely small sticking probability. Since their temperature range was limited to 77–400 K, it did not appear in their thermal desorption spectra, since desorption only takes place above 700 K.

Based on the results of Brill *et al.* (*10–12*), Ruch (*33*) proposed a model in which N_2 molecules are preferentially adsorbed on the

so-called C_7 sites (i.e., locations with seven neighboring Fe atoms) present on Fe(111). The π orbitals of N_2 were assumed to interact with empty Fe orbitals, thus leading to a weakening of the N–N bond which should be favorable for hydrogenation.

Evidence for the existence of a tightly bound molecular species on synthetic Fe ammonia catalysts is based on more or less indirect conclusions: Scholten *et al.* (*14*) suggested, from an analysis of their kinetic data, that adsorption is partly molecular above $\theta = 0.25$. From the amount of CO adsorbed on surfaces precovered with nitrogen, Takezawa and Emmett (*7*) concluded that complete dissociation occurs only above 700 K. Similar conclusions were drawn by Morikawa and Ozaki (*6*) from a comparison of the rates of nitrogen isotope exchange and displacement.

A detailed discussion of all these investigations would be far beyond the scope of the present work. It is only pointed out that the observed effects of surface–bulk segregation and reconstruction of the surface region certainly complicate the analysis of such data.

As a result of the present UPS measurements, there is clear *direct* evidence for the absence of appreciable amounts of nitrogen molecularly adsorbed on Fe(100) and Fe(111) at temperatures >140 K and pressures $<10^{-5}$ Torr. The main feature of the spectra (outside the d band) was the occurrence of a chemisorption-induced peak at about 5 eV below E_F, quite similar to the cases of Ni(111) (creation of N_{ad} by decomposition of NO and reduction of O_{ad} by hydrogen) (*26*) and Cu(100) (adsorption of atomic nitrogen) (*30*). This maximum is interpreted as arising from a bonding chemisorption level due to coupling of N 2p states to the metal. Eventually, the second maximum at -1.8 eV [Cu: -1.3 eV (*30*)] arises from an anti-bonding chemisorption level, but interpretation of spectral changes within the energy range of d-band emission is still rather uncertain. Anyway, as outlined in Section 3.5, the presence of N–N bonds should cause a spectrum similar to those from adsorbed CO, namely, with two maxima below the d band, which was never observed under the present conditions.

Further support for the atomic nature of the adsorbate stems from the isotopic exchange experiments, although this might not be considered as direct evidence, since dissociation might occur during heating the sample to the desorption temperature.

The weakly held electropositive species detected on Fe(111) at 140 K under a steady-state pressure of 4×10^{-4} Torr is identified with molecularly adsorbed nitrogen, in agreement with the general identification of this species (*20, 31, 32*), but without any direct evidence from UPS. For N_2/Fe, Beeck (*34*) derived a heat of adsorption of 10 kcal/mole, which agrees fairly well with Wedler's value for his γ state (5 kcal/mole) (*20*) and the estimates of the present work (5–10 kcal/mole). So far it is not clear whether this is a physisorbed state or a case of weak chemisorption. The observed difference between Fe(100) and Fe(111) probably favors the second explanation. Calculations by Doyen (*35*) suggest such a possibility, in which the axis of the N_2 molecule is directed perpendicular to the surface (similar to the case of CO chemisorption). It must further be kept in mind that, under the conditions of "real" ammonia synthesis (N_2 pressure in the order of 100 atm), even at 700 K, a species with a rather low adsorption energy will cover an appreciable part of the surface so that its participation in the reaction cannot be ruled out on the basis of such arguments.

4.2. Structure of the Surface Layer

With Fe(100), all the results from the different techniques point toward formation of a simple adsorbate overlayer, with-

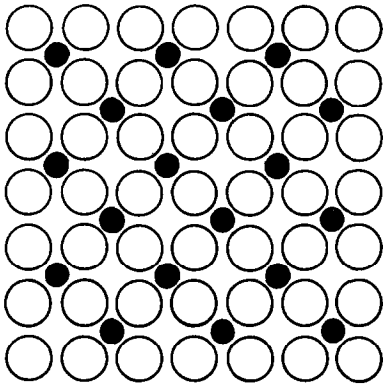

FIG. 16. Proposed model for the c2 × 2 structure formed on Fe(100) by nitrogen adsorption. Open circles: Fe atoms of the unreconstructed surface; filled circles: N atoms.

out any indication of displacement of the surface Fe atoms under the influence of the chemisorbed nitrogen atoms. A plausible model for the c2 × 2 structure is reproduced in Fig. 16. Although no detailed analysis of the LEED intensities was performed there is great evidence for the location of the N atoms in fourfold symmetric sites: (i) With only very few exceptions, all atomic adsorbates studied so far are located in the highest coordinated site on the surface (*36*). (ii) The same fourfold adsorption site was determined for N/Cu (100), where a c2 × 2 structure is also formed (*30*). (iii) The same location is attained by the N atoms in the bulk of (fcc) Fe_4N (*37*). In fact, the topmost layer of the c2 × 2-N/Fe(100) system corresponds closely to the (002) plane of this compound, and we believe this to be the main reason why the Fe(100) surface does not reconstruct. Obviously, the most stable configuration is already reached with this type of overlayer. Figure 17 shows the unit cell of Fe_4N (*38*), in which the Fe atoms form an fcc lattice with a nearest-neighbor distance of 2.68 Å, somewhat smaller than the distance between the atoms on the bcc-Fe(100) plane (2.86 Å). Taking into account the atomic radii of Fe (1.24 Å) and interstitial nitrogen [~0.7 Å (*38*)], a vertical distance for the adsorbed N atoms above the plane of the surface atoms of Fe(100) equal to about 0.6 Å is estimated on the basis of a hard-sphere model, i.e., the N atoms are somewhat protruding from the substrate layer in contrast to the situation with the corresponding plane in Fe_4N. [With N/Cu(100), Burkstrand *et al.* (*30*) originally derived a vertical distance of 1.4 Å, which, however, according to recent calculations, is more likely to be about 0.8 Å (*39*).] According to this model, each N atom would be in contact with five Fe atoms (with probably slightly unequal distances) of about 2.0 (±0.05) Å, whereas this distance in Fe_4N is 1.89 Å (*38*).

The completion of the c2 × 2 structure is equivalent to saturation of the Fe(100) surface due to interaction with N_2. The corresponding coverage is then $\theta = 0.5$ which may be used to calibrate the relative surface concentrations as obtained from the AES y values. Further uptake of nitrogen was observed under the electron beam, leading to splitting of the LEED "extra" spots. Obviously, the empty sites on the surface may be occupied by N atoms impinging from the gas phase, whereas N_2 presumably needs two neighboring vacant sites in order to chemisorb dissociatively.

With Fe(111), the surface structures are much more complicated, and the data suggest the reconstruction of the topmost atomic layers and the formation of coincidence lattices. This reconstruction certainly extends to only a very few atomic

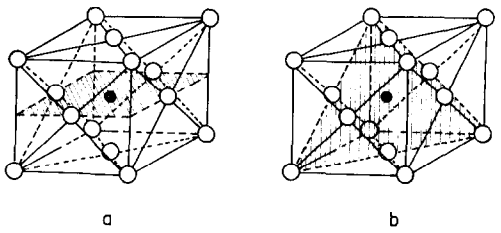

FIG. 17. Unit cell of fcc Fe_4N (*38*). Open circles: Fe atoms; filled circle: N atom; (a) (002) plane shaded; (b) (111) plane shaded.

layers, since both LEED and UPS still exhibit pronounced features from the metallic substrate. The mean free path of electrons with energy of about 30 eV (as used with LEED and UPS) is only about 5 Å (*47*), so that probably two or three atomic layers are involved in the reconstruction. (The AES data on the other hand already indicate appreciable damping of the Auger electrons emitted from the nitrogen atoms.) With the c2 × 2 structure on Fe(100), the distance between neighboring N atoms is 4.05 Å, which is also exactly the lateral interatomic separation between the topmost iron atoms on Fe(111). Therefore, the formation of a simple 1 × 1 structure by placing the adsorbate atoms in C_7 sites could probably be expected. The Fe–N distance within the Fe(111) plane, however, would then be more than 2.3 Å, which is considerably larger than that derived for Fe(100). This is presumably the reason why reorganization of the surface atoms in order to achieve better overlap of wave functions is energetically more favorable.

Following the conclusions for N/Fe(100), an interpretation in terms of analogies with iron nitrides again seems very reasonable.

TABLE 2

Two Possible Sets of Lattice Parameters (a) and Rotations (α) of the Unit Cell (with Respect to That of the Substrate Lattice) for a Hexagonal Arrangement of Fe Atoms on the Reconstructed Fe(111) Surface Which Would Give Rise to the Observed LEED Patterns

	Structure		a (Å)	α (degree)
Set A	3 × 3		2.648	10.9
	$19^{\frac{1}{2}} \times 19^{\frac{1}{2}}$	R 23.4°	2.689	15.8
	$21^{\frac{1}{2}} \times 21^{\frac{1}{2}}$	R 10.9°	2.676	40.9
	$3(3)^{\frac{1}{2}} \times 3(3)^{\frac{1}{2}}$	R 30°	2.691	3.67
	2 × 2		2.697	0
Set B	3 × 3		2.784	23.4
	$19^{\frac{1}{2}} \times 19^{\frac{1}{2}}$	R 23.4°	2.823	20.5
	$21^{\frac{1}{2}} \times 21^{\frac{1}{2}}$	R 10.9°	2.827	18.5
	$3(3)^{\frac{1}{2}} \times 3(3)^{\frac{1}{2}}$	R 30°	2.910	16.2
	2 × 2		3.03	19.1

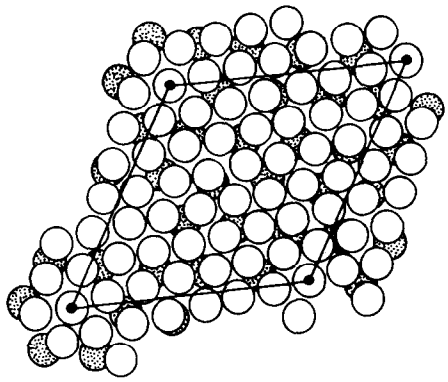

FIG. 18. Hexagonal arrangement of Fe atoms with a = 2.83 Å, the unit cell being rotated by 18.5° with respect to the Fe(111) substrate lattice, forming a coincidence structure which could account for the formation of the observed $21^{\frac{1}{2}} \times 21^{\frac{1}{2}}$ R 10.9° LEED pattern.

Discussion of the possible formation of "surface nitrides" on iron, even under conditions in which the known bulk nitrides are thermodynamically unstable, is not new (*8*, *18*, *40–42*), but was usually based on indirect conclusions from kinetic data. Below 590°C, besides the very limited solubility of nitrogen in α-Fe, essentially three different stable iron nitrides were found to exist (*38*): An fcc γ' phase with a rather narrow composition range around Fe_4N (*37*), an hcp ϵ phase extending from about Fe_3N up to nearly Fe_2N (*43*) and orthorhombic Fe_2N (*37*). In addition, several metastable structures have been investigated (*38*, *44*). From the symmetries of the LEED patterns and the derived unit cells (for the combined systems substrate +surface lattice), it must be concluded that "surface nitride" planes with hexagonal symmetry are formed. These could, for example, be the (111) plane of the γ' phase (Fe_4N) or the (0002) plane of the ϵ phase. The former has a lateral lattice constant of 2.683 Å (*37*), whereas, in the latter case, this quantity varies between 2.660 and 2.764 Å for N/Fe ratios between 0.24 and 0.49 (*43*). Several combinations of lattice constants and unit cell rotations were tested

to simulate the observed LEED patterns. Two sets of parameters, as shown in Table 2, were found to be nearly compatible with bulk nitride properties as well as with the observed LEED patterns. Set A would be based on the arrangement of Fe atoms like that in the (111) plane of Fe_4N, with nearly constant atomic separations which agree almost exactly with those in Fe_4N. The density of Fe atoms would be about 1.60 $\times 10^{15}$ cm^{-2}, compared to 0.70 $\times 10^{15}$ cm^{-2} with the unreconstructed Fe(111) surface. With set B, the lattice constant would continuously increase and would be slightly larger than the known values for bulk nitrides [as is also the case with the c2 $\times$ 2 structure on Fe(100)]. The density of Fe atoms in these planes would vary between 1.49 and 1.23 $\times 10^{15}$ cm^{-2}. Figure 18 shows as an example how superposing a hexagonal layer of Fe atoms with a = 2.83 Å rotated by 18.5°, over the bcc-Fe(111) surface, would lead to the coincidence lattice of the observed $21^{\frac{1}{2}} \times 21^{\frac{1}{2}}$ R 10.9° structure.

The 3 $\times$ 3 structure occurring at the lowest N_2 exposures is probably not reconstructed, but is a simple overlayer. This assumption would imply unusually long-ranging interactions between neighboring nitrogen atoms (12.1 Å). The formation of "intermediate" ϵ nitrides such as $Fe_{24}N_{10}$ with periodic arrangements of the N atoms, however, indicates also in the case of bulk compounds a remarkable tendency for long-range ordering of the nitrogen atoms. Unfortunately, additional quantitative analysis of the surface structures on Fe(111), based on the determination of the N content, is not possible. Probably, as in the case of Fe(100), the structures do not even agree completely with those of bulk nitrides, so that no further speculations on possible structure models will be made at the present stage. Even the thickness of the "surface-nitride" layer is unclear: If similar nitrogen "surface" concentrations on Fe(100) and Fe(111) are assumed (which appears to be reasonable) and if the surface structure in both cases is believed to be related to that of Fe_4N, then about *two* atomic nitrogen layers would result for Fe(111). Such a number appears to be plausible in view of the AES and TDS data. Since the Fe atoms are more densely packed in the (111) plane of γ' nitride than in that of metallic Fe, this effect would contribute further to a lowering of the "apparent" surface concentration, as probed by AES.

No completely satisfying explanation for the occurrence of the 2 $\times$ 2 structure may be offered. Since no significant amounts of nitrogen may be detected in this case by AES, it must be concluded that the surface layer consists essentially only of Fe atoms. The formation of a coincidence lattice from a fcc(111) plane with a = 2.697 Å (without rotation of the unit cell) could account for the LEED pattern. An alternative possibility consists again in an expanded lattice rotated with respect to the substrate plane. It has to be assumed that the N atoms are located *below* the topmost layer. The occurrence of such an *underlayer* structure has, for example, recently clearly been identified with the N/Ti system (*45*).

The UPS data indicate only relatively small alterations in the electronic densities of states of the Fe d band-region after the formation of the "surface nitrides" on Fe(100) and Fe(111). Unfortunately, we are not aware of any photoemission spectra from bulk iron nitrides. However, the results again indicate that the surface layers are very thin, and that obviously the metallic character of Fe is widely preserved. This means that the Fe–Fe distances are not strongly altered [as is evident in the case of Fe(100)], and there is no appreciable electron flow from Fe to N atoms. [The system O/Ni is an example of opposite nature (*46*).] The nearly equal desorption energies for N_2 from Fe(100) and Fe(111) again indicate a similar type of bonding of N atoms on both planes.

The activated kinetics of surface recon-

struction manifests itself not only in the fact that ordered LEED patterns are only formed after heat treatment, but also in the temperature dependence of the work function variation with exposure as reproduced in Fig. 9. Obviously, dissociative chemisorption of nitrogen *on* the Fe(111) surface causes a continuous increase of the work function which is presumably partly compensated by a small decrease in the work function due to surface reconstruction after a critical minimum surface concentration is reached. Superposition of both processes then will account for the flat maximum in the $\Delta\phi$ vs exposure curves above 410 K, which shifts toward lower exposures with increasing temperature since reconstruction is accelerated. Finally, reconstruction becomes so fast that the $\Delta\phi$ maximum is suppressed, and the final value is slightly smaller than that attained at lower temperatures. Below 410 K, obviously, surface reconstruction is very slow, which also agrees with LEED observations whereafter ordered structures are only formed above this temperature.

Reconstruction of iron surfaces under the influence of nitrogen also became evident in the work on small catalyst particles by Boudart *et al.* (*15*, *16*). Mainly on the basis of Mössbauer spectroscopic measurements, these authors concluded that ammonia treatment leads to the creation of C_7 sites [as present on Fe(111)]. The present results point into opposite directions, namely, that the sites present on the (100) plane are preserved, whereas those on the (111) surface are transformed into another atomic arrangement. Nevertheless, there is no disagreement on the phenomenological findings of both studies, namely, the occurrence of nitrogen-induced surface reconstruction. Quite recently, Löffler and Schmidt (*42*) have shown that high-temperature treatment of polycrystalline iron surfaces with ammonia may even cause extensive facetting which can be observed by scanning electron microscopy.

4.3. Kinetics of Adsorption and Desorption

Compared with other gas/metal systems the rate of dissociative nitrogen chemisorption on iron was found to be extremely small, which probably may only be compared with the equally slow uptake of oxygen by some semiconductor surfaces (*48*). Even if the activation energy for adsorption E^*_{ad} is taken into account, only a fraction of about 10^{-6} of those molecules the thermal energy of which exceeds E^*_{ad} are chemisorbed. Surprisingly, the same number was already estimated by Emmett and Brunauer (*49*) in their classical work on N_2 adsorption on Fe synthetic ammonia catalysts. One might speculate that only a special geometric configuration and/or state of internal excitation of the N_2 molecule during its collision with the surface will prevent it from being reflected, but certainly much more sophisticated experiments will be needed to answer this question.

The different initial activation energies [$E^*_{ad} \approx 0$ for Fe(111) and $\sim$5 kcal/mole for Fe(100)] are essentially responsible for the more rapid nitrogen uptake by the Fe(111) plane. If, as is generally accepted, nitrogen chemisorption is the rate-limiting step in ammonia synthesis, then this plane should be catalytically more active as was proposed by Brill *et al.* (*11*) (however, based on different arguments). That ammonia synthesis over iron is a structure-sensitive reaction was also concluded in the work by Boudart *et al.* (*15*). From an energetic standpoint, however, these differences are very small, particularly if the high strengths of the N–N and Fe–N bonds are taken into consideration. Another point concerns the variation of E^*_{ad} with coverage: Figure 3 shows that the "induced" heterogeneity of the Fe(100) single-crystal caused by increasing nitrogen surface concentration is of about the same order of magnitude as the difference in initial activation energies between Fe(100) and

Fe(111). The effect that E^*_{ad} increases continuously with coverage on an energetically *a priori* homogeneous surface has been ascribed by de Boer (*53*) to the continuous increase of the work function. This does not appear to be a satisfactory explanation, although, at least for Fe(100), no alternative may be offered at the moment.

The kinetics of nitrogen adsorption and desorption on iron catalysts has already been studied frequently in the past (*14*, *49–52*), and there are some remarkable similarities with the present results: Emmett and Brunauer (*49*) published a set of curves of the adsorbed amount vs N_2 exposure at different temperatures for a doubly promoted $Fe–Al_2O_3–K_2O$ catalyst which looks qualitatively nearly identical to those reproduced in Fig. 1a for Fe(100). In particular, also above 680 K the curves cross those taken at lower temperatures. Again a continuous increase of E^*_{ad} with surface concentration was observed, the lowest value, however, being 14.4 kcal/mole. This is also the reason why their exposure scale is considerably larger than those of Fig. 1a and b.

Whereas in the older literature (*49*, *50*) iron catalysts were reported to start to chemisorb N_2 at a measurable rate at about 200°C, Scholten *et al.* (*14*) found that careful reduction of the surface may lead to a considerable lowering of the activation energy. With a singly promoted $Fe–Al_2O_3$ catalyst, a linear increase in the activation energy with coverage up to about 23 kcal/mole was found, whereas extrapolation to $\theta = 0$ yielded a value of $E^*_{ad} = 5.2$ kcal/mole.

As outlined in Section 3.2, the mean activation energies for N_2 desorption from Fe(100) and Fe(111) were estimated to be 58 and 51 kcal/mole. Again these numbers agree quite well with literature data: Scholten *et al.* (*14*) derived an initial value of 55 kcal/mole and a continuous decrease with increasing coverage; Emmett and Brunauer (*49*) determined a mean value of 51 kcal/mole and Grabke (*56*), 48.6 kcal/mole. For the decomposition of NH_3 on Fe (where desorption of N_2 is obviously the rate-limiting step), Winter (*54*) reported an activation energy of 50 kcal/mole, almost exactly the same value (49.6 kcal/mole) determined 45 years later by Löffler and Schmidt (*42*). Love and Emmett (*54*) derived a value of 45 kcal/mole.

The latter authors also studied the thermal decomposition of iron nitrides and derived, for the reaction $Fe_4N \rightarrow Fe_{metal} + \frac{1}{2}N_2$, an activation energy of 50 kcal/mole. With this compound decomposition was observed to start around 750 K, whereas the ϵ phase ($Fe_3N \ldots Fe_2N$) decomposed much more rapidly. This temperature agrees with the onset of thermal N_2 desorption in the present experiments, which together with the similar activation energies and the structural information from LEED confirms the idea of the formation of a "surface nitride" closely related (but presumably not identical) to Fe_4N. Desorption of N_2 may then be regarded as being equivalent to decomposition of the "surface nitride." Presumably this process is not rate limited by surface diffusion and recombination of nitrogen atoms and involves, at least for Fe(111), the restoration of the unreconstructed lattice of the clean surface. Such a mechanism also simply accounts for the fact that desorption is obviously not a second-order, but a first-order, rate process.

Taking into account the activation energies for adsorption, nearly equal values for the strength of the metal–nitrogen bond on Fe(100) and Fe(111) (139 and 138 kcal/mole, respectively) are derived. The difference between both planes obviously exists nearly completely only with respect to the activation barrier, but not for the ground-state energy. These numbers are, on the other hand, also quite close to the M–N bond energy of the system N/Ni(111) for which a value of 135 kcal/mole was estimated (*26*).

Although the solubility of nitrogen in the

bulk is extremely small under the applied conditions (*23*, *57*), this process clearly manifested itself in the kinetics of nitrogen uptake, isotope exchange, and thermal desorption experiments as outlined in the preceding section. Grieveson and Turkdogan (*57*) demonstrated that, even at 1700 K and 1 atm of N_2, more than 30 min is needed to establish the equilibrium concentration in a depth of 3 mm, which corresponds to our sample thickness. Therefore, this equilibrium was certainly never reached in the present experiments, and that is why, instead, we attempted to establish reproducible starting conditions. Although with normal small catalyst particles this effect will certainly play no role under steady-state conditions, it might at least be partly responsible for the reported induction period for NH_3 formation on freshly reduced catalysts (*15*, *58*). If, in a thermal desorption experiment, the surface nitrogen is removed, dissolved nitrogen atoms will diffuse back to the surface and give rise to a continuous increase in N_2 desorption above 900 K. The bulk diffusion coefficient of N in Fe has an activation energy of 18.9 kcal/mole and attains, at this temperature, a value of about 10^{-7} cm^2/sec (*57*), so that a mean displacement of about 3×10^{-4} cm within 1 sec will result. This number yields at least a qualitative feeling for the sample depth which is involved in high-temperature desorption and isotopic exchange processes. The solubility at 900 K is about 0.01 atom%, so that such a layer would contain about 10^{15} N atoms, corresponding to a complete monolayer at the surface. It thus becomes understandable why comparable amounts of "surface" and "bulk" nitrogen are involved in transient thermal desorption.

5. SUMMARY

The main results are briefly summarized as follows: (i) Interaction of N_2 with Fe(100) and Fe(111) surfaces above room temperature leads to dissociative chemisorption. Evidence for a weakly held (molecular) species was only found with Fe(111) under a steady-state N_2 pressure of 4×10^{-4} Torr at the lowest attainable temperature (140 K). (ii) The activation energies for adsorption are about 5 and 0 kcal/mole at the clean Fe(100) and Fe(111) surfaces, respectively, and increase with increasing coverage in both cases. At 500 K, the initial rate of adsorption at Fe(111) exceeds that at Fe(100) by a factor of about 20. The sticking probabilities are in the range of 10^{-6} to 10^{-7} and, therefore, much smaller than those expected from a simple collision model. (iii) On Fe(100), saturation is reached by completion of a simple $c2 \times 2$-overlayer structure with $\theta = 0.5$. A model is proposed in which this structure is related to the (002) plane of Fe_4N. With Fe(111), the observation of a series of complex LEED patterns together with the TDS, $\Delta\phi$, and AES data suggest reconstruction of the surface and formation of "surface nitrides" with a thickness of about two atomic layers. Most probably these coincidence lattices are related to the (111) plane of Fe_4N. (iv) Desorption of N_2 is apparently a first-order rate process for which mean activation energies of 58 and 51 kcal/mole for Fe(100) and (111) were derived. These values are very similar to the data in the literature for the activation energy of decomposition of Fe_4N, suggesting identical rate-limiting steps for both types of reactions. Taking into account the activation energies for adsorption, practically equal values for the strength of the metal–nitrogen bond on both planes result, indicating that the crystallographic orientation of the surface mainly influences only the height of the activation barrier.

ACKNOWLEDGMENTS

We are very grateful to Dr. J. Küppers for helpful assistance with the UPS measurements. This work was completed while one of the authors (G. E.) was at the Division of Chemistry and Chemical Engineering, California Institute of Technology, whose generous support is gratefully acknowledged. M. G. is

grateful to the Fonds der Chemischen Industrie for granting a Liebig-Stipendium. Financial support was obtained from the Deutsche Forschungsgemeinschaft (SFB 128) and from the Max Buchner-Stiftung.

REFERENCES

1. Emmett, P. H., *in* "The Physical Basis for Heterogeneous Catalysis" (E. Drauglis and R. I. Jaffee, Eds.), p. 3. Plenum Press, New York, 1975.
2. Temkin, M., and Pyzhev, V., *Acta Physicochim.* **12**, 327 (1940).
3. Tamaru, K., *Trans. Faraday Soc.* **59**, 979 (1963).
4. Ozaki, A., Taylor, H., and Boudart, M., *Proc. Roy. Soc. (London) A* **258**, 47 (1960).
5. Kummer, J. T., and Emmett, P. H., *J. Chem. Phys.* **19**, 68 (1964).
6. Morikawa, Y., and Ozaki, A., *J. Catal.* **12**, 145 (1968).
7. Takezawa, N., and Emmett, P. H., *J. Catal.* **11**, 131 (1968).
8. Shachko, V. I., Fogel, Y. M., and Kolot, V. Y., *Kinet. Katal.* **7**, 734 (1966).
9. Schmidt, W. A., *Angew. Chem. Int. Ed. Engl.* **7**, 139 (1968).
10. Brill, R., Jiru, P., and Schultz, G., *Z. Phys. Chem. N. F.* **64**, 215 (1969).
11. Brill, R., Richter, E. L., and Ruch, E., *Angew. Chem.* **79**, 905 (1967).
12. Brill, R., *J. Catal.* **16**, 16 (1970).
13. Wedler, G., and Borgmann, D., *J. Catal.* **44**, 139 (1976) and references therein.
14. Scholten, J. J. F., Zwietering, P., Konvalinka, J. A., and de Boer, J. H., *Trans. Faraday Soc.* **55**, 2166 (1959).
15. Dumesic, J. A., Topsoe, H., Khammouma, S., and Boudart, M., *J. Catal.* **37**, 503 (1975).
16. Dumesic, J. A., Topsoe, H., and Boudart, M., *J. Catal.* **37**, 513 (1975).
17. Logan, S. R., Moss, R. L., and Kemball, C., *Trans. Faraday Soc.* **54**, 922 (1958).
18. Emmett, P. H., Hendricks, S. B., and Brunauer, S., *J. Amer. Chem. Soc.* **52**, 1456 (1930).
19. Tretyakov, I. I., *et al.*, *Akad. Nauk SSSR, Proc. Phys. Chem. Sect.* **175**, 651 (1967) [Engl. Transl.].
20. Wedler, G., Borgmann, D., and Geuss, K. P., *Surface Sci.* **47**, 592 (1975); see also for further references.
21. Ertl, G., Grunze, M., and Weiss, M., *J. Vac. Sci. Technol.* **13**, 314 (1976).
22. Conrad, H., Ertl, G., Küppers, J., and Latta, E. E., *Faraday Discuss. Chem. Soc.* **58**, 116 (1974).
23. Fast, J. D., "Interaction of Metals and Gases," Vol. 1. Academic Press, New York, 1965.
24. Grabke, H. J., personal communication.
25. Hansen, M., "Constitution of Binary Alloys." McGraw-Hill, London, 1958.
26. Conrad, H., Ertl, G., Küppers, J., and Latta, E. E., *Surface Sci.* **50**, 296 (1975).
27. Comrie, C. M., Weinberg, W. H., and Lambert, R. M., *Surface Sci.* **57**, 619 (1976).
28. Turner, D. W., Baker, A. D., Baker, C., and Brundle, C. R., "Molecular Photoelectron Spectroscopy." Wiley, London, 1970.
29. See for example: Gustafsson, T., Plummer, E. W., Eastman, D. E., and Freeouf, J. L., *Solid State Commun.* **17**, 391 (1975).
30. Burkstrand, J. M., Kleiman, G. G., Tibbetts, G. G., and Tracy, J. C., *J. Vac. Sci. Technol.* **13**, 291 (1976).
31. Ponec, V., and Knor, J., *J. Catal.* **10**, 73 (1968).
32. Gundry, P. M., Haber, J., and Tompkins, F. C., *J. Catal.* **1**, 363 (1962).
33. Ruch, E., *in* "Zehn Jahre Fonds der Chem. Industrie", p. 163. Düsseldorf, 1960.
34. Beeck, O., Cole, W. A., and Wheeler, A., *Discuss. Faraday Soc.* **8**, 314 (1950).
35. Doyen, G., Thesis. Universität München, München, 1975.
36. Demuth, J. E., *in* "Proceedings, 50th International Conference on Colloids and Surfaces." Academic Press, New York, in press.
37. Jack, K. H., *Proc. Roy. Soc. (London) A* **195**, 34 (1948).
38. Jack, K. H., *Proc. Roy. Soc. (London) A* **208**, 200 (1951).
39. van Hove, M., personal communication.
40. Logan, S. R., Moss, R. L., and Kemball, C., *Trans. Faraday Soc.* **54**, 922 (1958).
41. Roginskij, S. Z., Tretyakov, J. I., and Shekhter, A. B., *Dokl. Akad. Nauk SSSR* **91**, 881 (1953),
42. Löffler, D. G., and Schmidt, L. D., *J. Catal.* **44**, 244 (1976).
43. Jack, K. H., *Acta Crystallogr.* **5**, 404 (1952).
44. Jack, K. H., *Proc. Roy. Soc. (London) A* **208**, 216 (1951).
45. Shih, H. D., Jona, F., Jepsen, D. W., and Marcus, P. M., *Phys. Rev. Lett.* **36**, 798 (1976).
46. Conrad, H., Ertl, G., Küppers, J., and Latta, E. E., *Solid State Commun.* **17**, 497 (1975).
47. Ertl, G., and Küppers, J., "Low Energy Electron Diffraction and Surface Chemistry," p. 7. Verlag Chemie Weinheim, 1974.
48. See for example: Spicer, W. E., Lindau, I., Gregory, P. E., Garner, C. M., Pianetta, P., and Chye, P. W., *J. Vac. Sci. Technol.* **13**, 780 (1976).
49. Emmett, P. H., and Brunauer, S., *J. Amer. Chem. Soc.* **56**, 35 (1934).

50. Zwietering, P., and Roukens, J. J., *Trans. Faraday Soc.* **50,** 178 (1954).
51. Kwan, T., *J. Phys. Chem.* **60,** 1033 (1956).
52. Scholten, J. J. F., and Zwietering, P., *Trans. Faraday Soc.* **53,** 1363 (1957).
53. de Boer, J. H., *Advan. Catal.* **8,** 116 (1956).
54. Winter, E., *Z. Phys. Chem.* **B13,** 401 (1931).
55. Love, K. S., and Emmett, P. H., *J. Amer. Chem. Soc.* **63,** 3297 (1941).
56. Grabke, H. J., *Ber. Bunsenges.* **72,** 541 (1968).
57. Grieveson, P., and Turkdogan, E. T., *Trans. AIME* **230,** 1604 (1964).
58. Brill, R., and Kurzidim, J., *Colloq. Int. Centre Nat. Rech. Sic.* **187,** 99 (1969).